American Mineralogist, Volume 94, pages 899–904, 2009

Effects of hydration on thermal expansion of forsterite, wadsleyite, and ringwoodite at ambient pressure

Yu Ye,* Richard A. Schwering, and Joseph R. Smyth

Department of Geological Sciences, University of Colorado, Boulder, Colorado 80309, U.S.A.

Abstract

Single-crystal X-ray diffraction has been used to measure the thermal expansion coefficients of forsterite, wadsleyite, ringwoodite, and their hydrous forms at ambient pressure, from temperatures as low as 133 K to as high as 919 K. Second-order polynomial fitting to $\ln(V/V_0)$ vs. T was applied to derive the expansion coefficients in the form of $\alpha = a_1 \times T + a_0$. The single crystal of anhydrous wadsleyite persisted up to 859 K. Hydrous forsterite was observed to dehydrate at 919 K, whereas hydrous wadsleyite started to dehydrate at 655 K. The crystal of ringwoodite with 0.20 wt% broke down at 911 K, and the two ringwoodite samples with 0.74 and 2.4 wt% H_2O, were observed to break down with an irreversible unit-cell expansion at 808 and 606 K, respectively. From room temperature to high temperatures in this study, the mean thermal volume expansion coefficients are 36.4(5) and 38.1(9) $\times 10^{-6}$ K^{-1}, respectively, for anhydrous and hydrous forsterite; 28.5(5) and 35.8(8) $\times 10^{-6}$ K^{-1}, respectively, for the anhydrous and hydrous wadsleyite; 30.6(9), 35.2(15), and 34.9(7) $\times 10^{-6}$ K^{-1} for the samples of ringwoodite with 0.2, 0.74, and 2.4 wt% H_2O, respectively. Thus, forsterite, wadsleyite, and ringwoodite all have larger thermal expansion coefficients in their hydrous forms than in their anhydrous forms.

Keywords: Thermal expansion, forsterite, wadsleyite, ringwoodite, single crystal

Introduction

Approximately 65% of the total mass of the Earth is composed of silicate rock in the mantle and crust. Hydrogen in silicate minerals has very important effects on physical properties, such as melting temperature, density, rheology, elastic properties, and thermal expansion. Furthermore, even minor amounts of hydrogen in the mantle may play a key role in the development and evolution of the hydrosphere (Smyth and Jacobsen 2006; Bolfan-Casanova 2005). Water may be transported to the mantle transition zone (410–660 km) or deeper by subducted slabs in the form of dense hydrous magnesium silicates (DHMS) (Ohtani et al. 2001; Inoue et al. 2004), as well as by hydrogen incorporated into nominally anhydrous phases, such as pyroxene, olivine, and garnet.

Olivine, wadsleyite, and ringwoodite, thought to be the major minerals in the upper mantle and transition zone, are nominally anhydrous, but can incorporate significant amounts of hydrogen in the form of hydroxyl in their crystal structures: Smyth (1987, 1994) predicted by theoretical studies that wadsleyite might contain up to 3.3 wt% H_2O. Inoue et al. (1995) subsequently synthesized pure wadsleyite (Mg_2SiO_4) with 3.3 wt% H_2O. Impure ringwoodite $(Mg, Fe)_2SiO_4$ was also shown to be able to contain up to about 3 wt% H_2O (Kohlstedt et al. 1996). Smyth et al. (2006) reported olivines with up to about 0.9 wt% H_2O synthesized at 12 GPa and 1523 K. To understand the role of nominally anhydrous silicates in the overall hydrogen budget of the planet, it is necessary to constrain the effects of hydration on the equations of state of the major phases of the interior. Constraining the effects of hydration on the thermal expansion of these phases may thus improve estimates of water contents in various regions of the interior. This study was conducted at ambient pressure, the first step in a study of the effects of hydration on thermal expansion. Further steps will be necessary in the future to constrain the thermal expansion at high pressures.

In addition to measurement of thermal expansion, high-temperature experiments on these phases may improve the understanding of breakdown mechanisms and dehydration kinetics. Anhydrous wadsleyite and anhydrous ringwoodite were observed to transform into forsterite at 1073 K (Inoue et al. 2004). Suzuki et al. (1979) reported the persistence of anhydrous ringwoodite up to 1023 K, and Suzuki et al. (1980) reported the back-transformation of anhydrous wadsleyite to forsterite at 1173 K. The thermal expansion of hydrous and anhydrous wadsleyite and ringwoodite above room temperature were studied by Inoue et al. (2004) by powder X-ray diffraction measurements performed at ambient pressure. The thermal expansion of hydrous forsterite, however, has not yet been reported.

In the current study, single-crystal X-ray diffraction was used to measure the thermal expansion of hydrous and anhydrous forsterite, wadsleyite, and ringwoodite from temperatures as low as 133 K to high temperatures of about 900 K. The e.s.d. values in the cell parameters and volume of this study are smaller than those of previous studies from X-ray powder diffraction. The thermal expansion coefficients were compared with the results from Inoue et al. (2004) and Suzuki et al. (1979, 1980), and a second-order polynomial fitting method was applied to $\ln(V/V_0)$ vs. T from low to high temperatures.

* E-mail: yey@colorado.edu

0003-004X/09/0007–899$05.00/DOI: 10.2138/am.2009.3122

EXPERIMENTAL METHODS

Sample synthesis

The samples of hydrous and anhydrous forsterite, wadsleyite, and ringwoodite were synthesized at Bayerisches Geoinstitut, Universität Bayreuth, Germany. The synthesis of hydrous forsterite was carried out in a double capsule experiment in the 5000 ton multi-anvil press at 12 GPa and 1523 K (Smyth et al. 2006). Water content was determined by polarized FTIR spectra on grains previously oriented by X-ray single-crystal measurements, using the calibration of Bell et al. (2003). Hydrous wadsleyite was synthesized at 17.5 GPa and 1673 K. Crystal structures and compressibilities of hydrous wadsleyite samples are reported by Holl et al. (2008). Anhydrous wadsleyite was synthesized at 18 GPa and 1773 K. The water contents of wadsleyite were determined from the *b/a* unit-cell ratio, according to the calibration of Jacobsen et al. (2005). The synthesis experiment of the ringwoodite with 0.74 wt% H_2O was conducted at 21.5 GPa and 1773 K, whereas the ringwoodite with 0.20 wt% H_2O was synthesized at 21 GPa and 1773 K. Water contents of these two samples were estimated from unpolarized FTIR spectra, using the calibration of Paterson (1982) at 0.20 and 0.74 wt% H_2O, respectively (Smyth et al. 2003). The ringwoodite with 2.4 wt% H_2O was synthesized at 20 GPa and 1523 K and the water content estimated from the unit-cell parameter (Smyth and Jacobsen 2006).

X-ray single-crystal diffraction

The X-ray data for anhydrous and hydrous forsterite, wadsleyite, and ringwoodite were collected at the Mineral Physics and Crystallography Lab, Department of Geological Science, University of Colorado at Boulder. A Bruker APEX2 CCD detector system was used to find the orientation matrices of the single crystals. Subsequently, measurements from a point detector system were used to refine the cell parameters. Both detectors are mounted on Bruker P4 four-circle diffractometers on an 18 kW rotating Mo-anode X-ray generator. The unit-cell parameters were refined by least-squares refinement of the data from the point detector. Mo radiation was used ($K\alpha_1 = 0.709300$ Å and $K\alpha_2 = 0.713590$ Å). $K\alpha(\text{mix}) = 0.71093$ Å, determined by the percentages of $K\alpha_1$ and $K\alpha_2$. We used a perfect single crystal of ruby with a near sphere shape to calibrate the $K\alpha$(mix), i.e., the wavelength used for all cell refinement. The 2θ range for all reflections was limited to 12 to 30°, because for angles larger than 30°, the reflected rays might have been blocked by the heater device before they reached the detector, and for these silicate samples, most of the strong reflections are within 2θ range of 12 to 30°, calculated by the wavelength of $K\alpha$(mix). This method is also consistent with our procedures in the high-pressure diamond cells. The generator voltage was 50 kV and the current 250 mA for all experiments. For low-temperature experiments, the single crystals were mounted on glass fibers and cooled down to temperatures as low as 133 K. Low temperatures were measured and controlled by an LT-2A controller, which uses a low-temperature N_2 gas stream. For high-temperature experiments, the crystals were mounted inside silica glass capillaries heated to temperatures as high as 919 K with a Bruker high-temperature device, which uses a two-prong ceramic-coated Pt wire radiant heater, with an Omega temperature-control unit. Measurements were generally conducted every 50 K for both low- and high-temperature runs.

There were differences between the real temperatures at the crystal positions and the temperatures read from the devices during the diffraction experiments because the tip of the thermocouple was 2–3 mm distant from the crystal. To determine the real temperatures of the sample more accurately, after the diffraction measurements were completed for each sample, an Omega calibrated chromel-alumel thermocouple was placed at the crystal position and read by an Omega CL3515R calibrator at every temperature at which diffraction measurements had been carried out. Throughout the low-temperature runs, the temperature values read from the Bruker LT-2A controller varied within a range of ±2 K about the set points. The systematic differences between the controller and the thermocouple calibrator were also within about 2 K. Thus the low temperatures, read from the controller were used in the following discussion, assuming an estimated uncertainty of ±2 K and ignoring any systematic offset. For the high-temperature runs, the high-temperature device gave a variation of ±5 K about each set point. The temperatures read from the calibrator were systematically as much as 17 K lower than those determined from the high-temperature device. Thus, the high temperatures reported in the following discussion are the values from the calibrator, instead of from the high-temperature device, assuming the uncertainty of ±5 K.

Calculation of thermal expansion coefficients

The thermal expansion coefficient, α, in units of K^{-1}, is defined by:

$$\alpha = 1/V\,(\partial V/\partial T)_p = (\partial \ln V/\partial T)_p. \quad (1)$$

In this study, the temperature dependence of α is expressed as

$$\alpha = a_1 \times T + a_0. \quad (2)$$

From Equations 1 and 2, $\ln(V/V_0)$ can be derived:

$$\ln(V/V_0) = \tfrac{1}{2}a_1 \times T^2 + a_0 \times T + b. \quad (3)$$

For each of the seven samples, V_0 is defined as the unit-cell volume at the lowest experimental temperature, T_0, so that the values of $\ln(V/V_0) \geq 0$ for all temperatures. The constant of integration, b, is determined by the value of V_0 and is not needed to calculate α. From Equation 3, a_0 and a_1 can be determined when fitting $\ln(V/V_0)$ vs. T to a second-order polynomial. These values are then used in Equation 2 to determine α.

Because the mean thermal expansion coefficient, α_0, is a commonly used measure, we put α_0 into Equation 1 and integrate:

$$\ln(V/V_0) = \alpha_0 \times T + C \quad (4)$$

where C is an integration constant. This is the method we used to calculate the mean thermal expansion coefficients α_0.

The software package Origin Professional 7.5 was used to perform linear fitting, and to calculate the slopes of the fitting lines, which gives the thermal expansion coefficients and their associated e.s.d. values.

RESULTS AND DISCUSSION

Thermal expansion of hydrous and anhydrous forsterite

All diffraction data of anhydrous and hydrous (0.89 wt% H_2O) forsterite are consistent with space group *Pbnm*. The experimental temperature range for anhydrous forsterite was from 153 to 889 K [$V_0 = 289.25(2)$ Å^3 at $T = 153$ K]. For hydrous forsterite, the temperature range was from 133 to 919 K [$V_0 = 289.54(2)$ Å^3 at $T = 133$ K]. We assume that hydrous forsterite dehydrated at about 919 K, as we observed an abrupt and irreversible decrease in the length of the *b* axis. Dehydration is assumed because at every temperature from 300 to 889 K measured in this study, the *b* axis of hydrous forsterite was about 0.01 Å larger than that of anhydrous forsterite. The dehydration was observed to be essentially complete in <10 min. That is because the measurement, which took about 1 h, was conducted 10 min after the temperature reached 919 K, while no evidence for further dehydration during the measurement at 919 K was observed, as all reflections recorded at this temperature were sharp and distinct. The crystal broke down after the measurement at 919 K. Hence, further experiments could not be conducted.

The unit-cell parameters and volumes of anhydrous and hydrous forsterite are listed in Appendix Tables 1[1] and 2[1], respectively. The thermal expansions of the *a*, *b*, and *c* axes are plotted in Figures 1a–1c. The functions $\ln(V/V_0)$ vs. T are plotted in Figure 2, where a second-order polynomial fitting is applied. The calculated a_1, a_0, and b, as defined in Equations 2 and 3, are listed in Table 1. The temperature range used for the second-order polynomial fit to the hydrous forsterite data were limited to temperatures below the dehydration (i.e., 133–889 K).

[1] Deposit item AM-09-030, Appendix Tables 1–5. Deposit items are available two ways: For a paper copy contact the Business Office of the Mineralogical Society of America (see inside front cover of recent issue) for price information. For an electronic copy visit the MSA web site at http://www.minsocam.org, go to the American Mineralogist Contents, find the table of contents for the specific volume/issue wanted, and then click on the deposit link there.

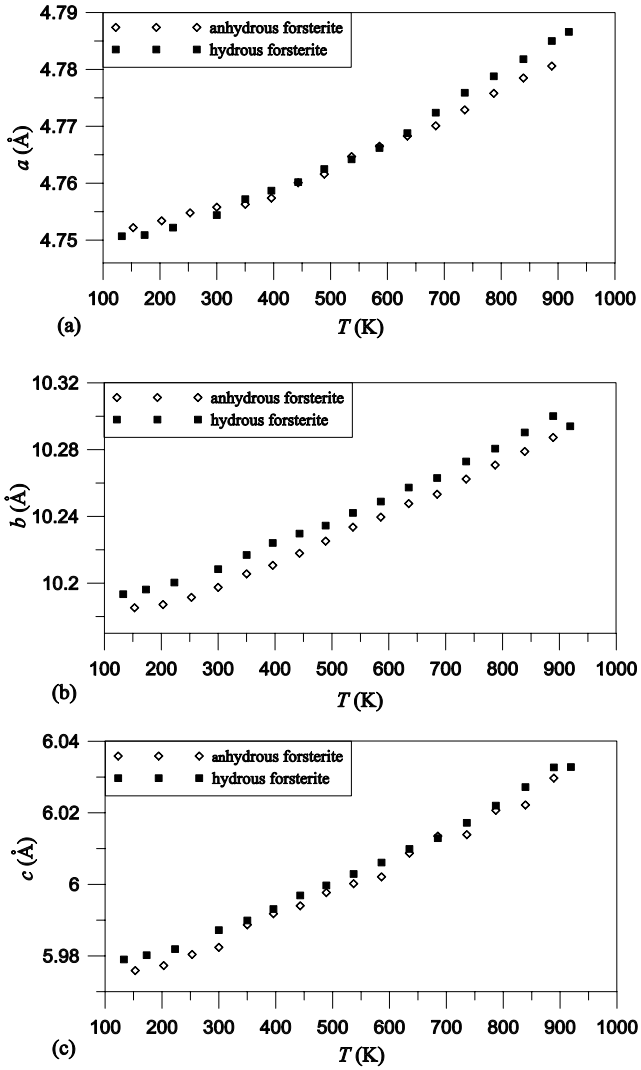

FIGURE 1. Temperature dependence of (**a**) the *a*, (**b**) the *b*, and (**c**) the *c* axes of anhydrous and hydrous (0.89 wt% H_2O) forsterite.

The values of the mean volume thermal expansion coefficients, α_0, for anhydrous and hydrous forsterite are listed in Table 2, and the calculated mean thermal expansion coefficients for the *a*, *b*, and *c* axes are given in Table 3.

Thermal expansion of anhydrous and hydrous wadsleyite

The diffraction patterns of both anhydrous and hydrous (2.1 wt% H_2O) wadsleyite are consistent with space group *Imma* (Holl et al. 2008). Both anhydrous and hydrous wadsleyite were cooled down to a temperature of 153 K, where V_0 = 537.46(10) and V_0 = 538.53(15) Å^3 for anhydrous and hydrous wadsleyite, respectively. Anhydrous wadsleyite was heated to 859 K, at which point the single crystal broke down.

We interpret the onset of dehydration of hydrous wadsleyite as occurring at 655 K, the temperature at which an abrupt increase in the *a* cell edge and an abrupt decrease of the *b* cell edge were observed (Fig. 3). The change is attributed to dehydration, because anhydrous wadsleyite has a longer *a* axis and a shorter *b* axis than hydrous wadsleyite. There is not much difference between the *c* axes of the two samples. Liu et al. (1998) reported that hydrous wadsleyite converted to a defective forsterite at 723 K in about 5 min, while Inoue et al. (2004) observed that hydrous wadsleyite began dehydration at 723 K.

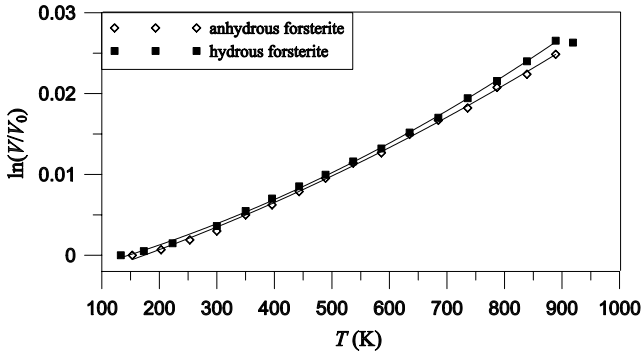

FIGURE 2. Temperature dependence of $\ln(V/V_0)$ of anhydrous and hydrous (0.89 wt% H_2O) forsterite. The second-order polynomial curves are over the range 153 to 889 K for anhydrous forsterite (R^2 = 0.9988) and 133 to 889 K for hydrous forsterite (R^2 = 0.9994).

TABLE 1. The values of the coefficients a_1, a_0, and *b* derived from the second-order polynomial fits to $\ln(V/V_0)$ for anhydrous and hydrous forms of forsterite, wadsleyite, and ringwoodite

	a_1 (10^{-8})	a_0 (10^{-4})	*b* (10^{-3})	*T* range (K)
anhydrous forsterite	2.4(3)	0.219(17)	–4.2(4)	153–889
hydrous forsterite	3.4(2)	0.178(11)	–3.0(2)	133–889
anhydrous wadsleyite	2.2(3)	0.16(2)	–3.1(3)	133–808
hydrous wadsleyite	7.5(10)	0.02(8)	–1.2(7)	133–606
ringwoodite I	3.6(2)	0.104(10)	–1.9(2)	133–859
ringwoodite II	6.2(4)	0.02(2)	–7(4)	133–777
ringwoodite III	8.0(8)	0.02(2)	–8(4)	133–577

The unit-cell parameters and volumes of anhydrous and hydrous wadsleyite are listed in Appendix Tables 3[1] and 4[1], respectively. The thermal expansion of the *a*, *b*, and *c* axes are plotted in Figures 3a–3c. The functions $\ln(V/V_0)$ vs. *T* are plotted in Figure 4, where a second-order fit is applied. The calculated values of a_1, a_0, and *b* are listed in Table 1. The temperature range used for the second-order polynomial fit of hydrous wadsleyite data was restricted to temperatures before the dehydration (i.e., 133–606 K). Hydrous wadsleyite has a large e.s.d. associated with a_0, and a_0 is also smaller for hydrous than for anhydrous wadsleyite.

The values of α_0 for anhydrous and hydrous wadsleyite are listed in Table 2, and the mean thermal expansion coefficients for *a*, *b*, and *c* axes are given in Table 3.

Thermal expansion of ringwoodite

In this study, three different samples of hydrous ringwoodite were used with 0.20, 0.74, and 2.4 wt% H_2O. We refer to them here as ringwoodite I, II, and III, respectively, in the order of increasing water content. The diffraction patterns of all three samples are consistent with space group *Fd*3*m*. Each of the three samples was cooled to a temperature of 133 K, where values of V_0 of 523.27(12), 523.86(6), and 526.76(16) Å^3 were determined for ringwoodite I, II, and III, respectively. Ringwoodite I was heated to 911 K, where the volume of the unit cell increased abruptly. At this temperature, significantly broadened reflections were observed, and this was reflected in the larger e.s.d. of the unit-cell volume, relative to those determined at lower temperatures. The crystal was then moved back to the APEX2 CCD detector to collect another diffraction pattern at room

TABLE 2. The linear thermal volume expansion coefficients of anhydrous and hydrous forms of forsterite, wadsleyite, and ringwoodite

	H_2O (wt%)	α_0(10^{-6} K^{-1})	*T* range (K)	Ref
anhydrous forsterite	0	36.4(5)	300–889	This study
	0	34.3(6)	303–1173	Suzuki (1975)
hydrous forsterite	0.89	38.1(9)	300–889	This study
anhydrous wadsleyite	0	28.5(5)	303–808	This study
	0	34.0(5)	293–973	Inoue et al. (2004)
	0	29.4(8)	293–1073	Suzuki et al. (1980)
hydrous wadsleyite	2.1	35.8(14)	303–606	This study
	2.4(2)	30.1(14)	303–623	Inoue et al. (2004)
ringwoodite	0	30.7(6)	293–973	Inoue et al. (2004)
	0	24.7(5)	293–1023	Suzuki et al. (1979)
I:	0.2	30.6(9)	303–859	This study
II:	0.74	35.2(15)	303–777	This study
III:	2.4	34.9(7)	303–577	This study
	2.6(3)	27.3(9)	303–623	Inoue et al. (2004)

temperature. The pattern observed was that of a polycrystalline powder, which indicated that the crystal was still ringwoodite, but had begun to break down. The data taken below 911 K were used for calculation in the following discussion.

Liu et al. (2002) reported that hydrous ringwoodite sometimes converts to a defective forsterite structure above 900 K. Inoue et al. (2004) reported that dehydration of hydrous ringwoodite powder starts at 723 K by observations of a decrease in the unit-cell volume. However, in the current study, breakdown of the two hydrous samples was observed as irreversible expansions of the unit cells above certain temperatures. For ringwoodite II, the temperature of irreversible expansion was 808 K. The volume of the unit cell after having been heated to 808 K and cooled to room temperature was 532.1(5) $Å^3$, whereas the initial room temperature volume was 525.86(6) $Å^3$. The temperature of irreversible expansion for ringwoodite III was 606 K. The volume of the unit cell after having been heated to 606 K and cooled to room temperature was 530.55(7) $Å^3$, while the initial room temperature volume was 528.16(6) $Å^3$. In contrast to dehydration of hydrous wadsleyite discussed above, irreversible expansions of the unit cell were observed for ringwoodite II and III. This irreversible expansion is clearly a metastable phenomenon associated with breakdown and possible back transformation of the ringwoodite well outside its field of stability. Like ringwoodite I, ringwoodite II and III were not single crystals after the high-temperature measurements. Hence, we could not determine the water contents for ringwoodite II and III after the experiments. In the following calculation of the thermal expansion coefficients of both ringwoodite II and III, the temperature ranges chosen for the fits are cut off just below the temperatures of irreversible expansion.

The unit-cell parameters and volumes of all samples are listed in Appendix Table 5[1]. The functions $\ln(V/V_0)$ vs. T are plotted in Figure 5, where a second-order fit is applied. The calculated values of a_1, a_0, and b are listed in Table 1. The values of α_0 for the three samples are listed in Table 2. As is the case for hydrous wadsleyite, the values of a_0 for ringwoodite II and III are smaller than that of ringwoodite I and have large associated e.s.d. values.

TABLE 3. The mean thermal expansion coefficients of *a*, *b*, and *c* axes of anhydrous and hydrous forms forsterite and wadsleyite

	α_0 (*a*) (10^{-6} K^{-1})	α_0 (*b*) (10^{-6} K^{-1})	α_0 (*c*) (10^{-6} K^{-1})	Ref
anhydrous forsterite	9.2(2)	14.8(1)	12.5(4)	This study
	9.2(3)	13.4(2)	11.7(3)	Suzuki (1975)
hydrous forsterite	10.8(4)	14.7(3)	12.5(3)	This study
anhydrous wadsleyite	7.6(3)	7.1(3)	14.0(3)	This study
	8.7(2)	11.6(5)	13.7(2)	Inoue et al. (2004)
	9.1(6)	6.9(7)	13.5(6)	Suzuki et al. (1979)
hydrous wadsleyite	8.4(3)	11.0(7)	16.4(10)	This study
	9.7(7)	*	18(2)	Inoue et al. (2004)

*The data for the *b* axis are not good enough to determine α_0 (*b*) well.

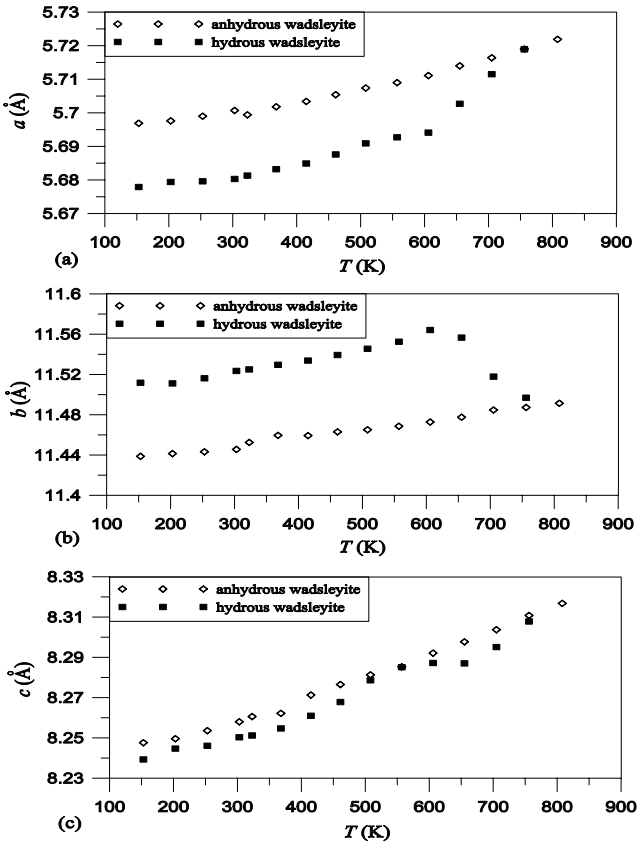

FIGURE 3. Temperature dependence of (**a**) the *a*, (**b**) the *b*, and (**c**) the *c* axes of anhydrous and hydrous (2.1 wt% H_2O) wadsleyite.

Effects of hydration on thermal expansion

From Table 2, the trend across the seven samples of forsterite, wadsleyite, and ringwoodite is that the mean volume thermal expansion coefficient, α_0, is larger for the hydrous than the anhydrous forms. Using Raman spectroscopy at ambient pressure, Liu et al. (1998, 2002) reported that both hydrous wadsleyite and hydrous ringwoodite have volume thermal expansion coefficients that are slightly smaller than those of the corresponding anhydrous forms. A similar conclusion was reached by Inoue et al. (2004), using high-temperature powder X-ray diffraction at ambient pressure. For ringwoodite II and III, the values of α_0 are calculated from the data taken below their temperatures of irreversible expansion. Ringwoodite III has a lower temperature of irreversible thermal expansion than ringwoodite II. Data for ringwoodite III was fit over the temperature range of 303–577 K,

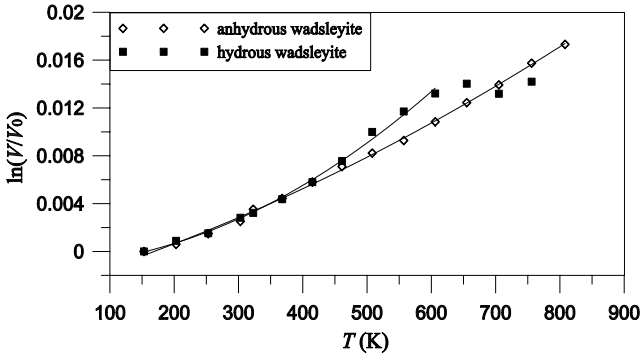

FIGURE 4. Temperature dependence of $\ln(V/V_0)$ of anhydrous wadsleyite and hydrous (2.1 wt% H_2O) wadsleyite. The second-order polynomial curves are from 133 to 808 K for anhydrous wadsleyite (R^2 = 0.9987) and from 133 to 606 K for hydrous wadsleyite (R^2 = 0.9962).

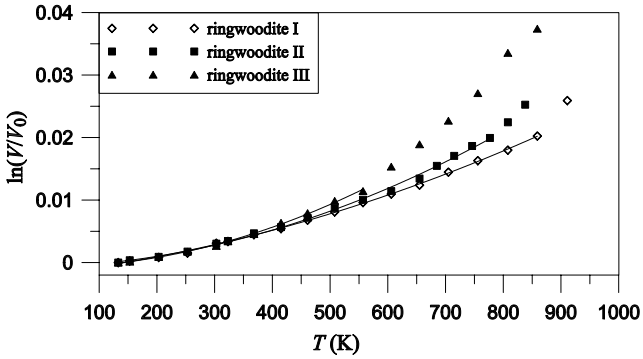

FIGURE 5. Temperature dependence of $\ln(V/V_0)$ of ringwoodite I, II, and III, with 0.20, 0.74, and 2.4 wt% H_2O, respectively. The second-order polynomial curves are from 133 to 859 K for ringwoodite I (R^2 = 0.9992), from 133 to 777 K for ringwoodite II (R^2 = 0.998), and from 133 to 577 K for ringwoodite III (R^2 = 0.9981).

while that for ringwoodite II was fit over the range of 303–777 K. From such fits, the calculated α_0 for ringwoodite III is smaller than that of ringwoodite II.

The data from this study have smaller e.s.d. values associated with the unit-cell parameters and volumes, and are less scattered than those of Inoue et al. (2004). In Figures 1–5, the error bars for the unit-cell parameters and $\ln(V/V_0)$ are smaller than the sizes of the symbols. The second-order polynomial fits applied to these seven silicates accurately describe the results, with R^2 close to 1. All hydrous samples of forsterite, wadsleyite, and ringwoodite have larger values of a_1 than their corresponding anhydrous forms. The values of a_0 are much smaller for the hydrous ringwoodite and wadsleyite than those of their corresponding anhydrous forms. In addition, the rapid dehydration observed in forsterite above 900 K may explain why natural olivines with more than about 200 ppm H_2O have not been observed.

In these experiments, we have constrained the effects of hydration on thermal expansion at ambient pressure of the three most abundant phases of the upper mantle and transition zone. We observe a systematic increase in thermal expansion with hydration in all three phases. This is consistent with volume expansions observed with hydration at ambient temperature and pressure (Smyth et al. 2003, 2006; Jacobsen et al. 2006). The hydration mechanism in all three appears to be predominantly octahedral site vacancy with protons located in the periphery of the vacant octahedra (Hushur et al. 2009; Holl et al. 2008; Smyth et al. 2003). Decreased bond strength around the vacant octahedra is then expected to result in increased thermal expansivity in each of these phases with hydration. This vacancy mechanism is also consistent with the ambient pressure and temperature volume expansion and decreased bulk and shear moduli observed with hydration in these phases (Jacobsen et al. 2008; Mao et al. 2008; Jacobsen and Smyth 2006). To map out hydration in the upper mantle and transition zone, however, it will be necessary to constrain thermal expansion at pressure or elastic properties at both elevated temperature and pressure in hydrated samples. We hope the current study is a significant step in this process.

ACKNOWLEDGMENTS

This study was supported by U.S. National Science Foundation grant EAR07-11165. Sample synthesis was supported in part by Bayerisches Geoinstitut Visitors Program and the Alexander von Humboldt Foundation.

REFERENCES CITED

Bell, D.R., Rossman, G.R., Maldener, J., Endisch, D., and Rauch, F. (2003) Hydroxide in olivine: A quantitative determination of the absolute amount and calibration of the IR spectrum. Journal of Geophysical Research, 108, 2105, DOI: 10.1029/2001JB000679.

Bolfan-Casanova, N. (2005) Water in the Earth's mantle. Mineralogical Magazine, 69, 229–257.

Holl, C.M., Smyth, J.R., Jacobsen, S.D., and Frost, D.J. (2008) Effects of hydration on the structure and compressibility of wadsleyite, β-(Mg_2SiO_4). American Mineralogist, 93, 598–607.

Hushur, A., Manghnani, M.H., Smyth, J.R., Nestola, F., and Frost, D.J. (2009) Crystal chemistry of hydrous forsterite and its vibrational properties up to 41 GPa. American Mineralogist, 94, 751–760.

Inoue, T., Yurimoto, H., and Kudoh, Y. (1995) Hydrous modified spinel, $Mg_{1.75}SiH_{0.5}O_4$: A new water reservoir in the mantle transition region. Geophysical Research Letters, 22, 117–120.

Inoue, T., Tanimoto, Y., Irifune, T., Suzuki, T., Fukui, H., and Ohtaka, O. (2004) Thermal expansion of wadsleyite, ringwoodite, hydrous wadsleyite, and hydrous ringwoodite. Physics of the Earth and Planetary Interiors, 143–144, 279–290.

Jacobsen, S.D. and Smyth, J.R. (2006) Effect of water on the sound velocities of ringwoodite in the transition zone. In S.D. Jacobsen and S. van der Lee, Eds., Earth's Deep Water Cycle, 168, p. 131–145. Monograph Series, American Geophysics Union, Washington, D.C.

Jacobsen, S.D., Demouchy, S., Frost, D.J., Boffa-Ballaran, T., and Kung, J. (2005) A systematic study of OH in hydrous wadsleyite from polarized FTIR spectroscopy and single-crystal X-ray diffraction: Oxygen sites for hydrogen storage in the Earth's interior. American Mineralogist, 90, 61–70.

Jacobsen, S.D., Jiang, F., Mao, Z., Duffy, T.S., Smyth, J.R., Holl, C.M., and Frost, D.J. (2008) Effects of hydration on the elastic properties of olivine. Geophysical Research Letters, 35, L14303.

Kohlstedt, D.L., Keppler, H., and Rubie, D.C. (1996) Solubility of water in the α, β, and γ phases of $(Mg,Fe)_2SiO_4$. Contributions to Mineralogy and Petrology, 123, 345–357.

Liu, L.-G., Mernagh, T.P., Lin, C.-C., Xu, J.-A., and Inoue, T. (1998) Raman spectra of hydrous β-Mg_2SiO_4 at various pressures and temperatures. In M.H. Manghnani and T. Yagi, Eds., Properties of Earth and Planetary Materials at High Pressure and Temperature, 101, p. 523–530. Geophysical Monograph, American Geophysics Union, Washington, D.C.

Liu, L.-G., Lin, C.-C., Mernagh, T.P., and Inoue, T. (2002) Raman spectra of hydrous γ-Mg_2SiO_4 at various pressures and temperatures. Physics and Chemistry of Minerals, 29, 181–187.

Mao, Z., Jacobsen, S.D., Jiang, F., Smyth, J.R., Holl, C.M., and Duffy, T.S. (2008) Single-crystal elasticity of wadsleyites, β-Mg_2SiO_4, containing 0.37–1.66 wt% water. Earth and Planetary Science Letters, 268, 540–549.

Ohtani, E., Toma, M., Litasov, K., Kubo, T., and Suzuki, A. (2001) Stability of dense hydrous magnesium silicate phases and water storage capacity in the transition zone and lower mantle. Physics of the Earth and Planetary Interiors, 124, 105–117.

Paterson, M.S. (1982) The determination of hydroxyl by infrared absorption in quartz, silicate glasses and similar materials. Bulletin Minéralogique, 105, 20–29.

Smyth, J.R. (1987) β-Mg_2SiO_4: A potential host for water in the mantle? American

Mineralogist, 72, 1051–1055.
——— (1994) A crystallographic model for hydrous wadsleyite: An ocean in the Earth's interior? American Mineralogist, 79, 1021–1025.
Smyth, J.R. and Jacobsen, S.D. (2006) Nominally anhydrous minerals and Earth's deep water cycle. In S.D. Jacobsen and S. van der Lee, Eds., Earth's Deep Water Cycle, 168, p. 1–11. Monograph Series, American Geophysical Union, Washington, D.C.
Smyth, J.R., Holl, C.M., Frost, D.J., Jacobsen, S.D., Langenhorst, F., and McCammon, C.A. (2003) Structural systematics of hydrous ringwoodite and water in Earth's interior. American Mineralogist, 88, 1402–1407.
Smyth, J.R., Frost, D.J., Nestola, F., Holl, C.M., and Bromiley, G. (2006) Olivine hydration in the deep upper mantle: Effects of temperature and silica activity. Geophysical Research Letters, 33, L15301.
Suzuki, I. (1975) Thermal expansion of periclase and olivine and their anharmonic properities. Journal of Physics of the Earth, 23, 145–159.
Suzuki, I., Ohtani, E., and Kumazawa, M. (1979) Thermal expansion of γ-Mg_2SiO_4. Journal of Physics of the Earth, 27, 53–61.
——— (1980) Thermal expansion of modified spinel, β-Mg_2SiO_4. Journal of Physics of the Earth, 28, 273–280.

Manuscript received October 20, 2008
Manuscript accepted February 6, 2009
Manuscript handled by Ian Swainson